CrystEngComm

PAPER

View Article Online
View Journal | View Issue

Cite this: *CrystEngComm*, 2025, **27**, 5625

Transformation of carbon dioxide catalyzed using an N-heterocyclic carbene copper(I)-embedded metal–organic framework†

Li-Xin You, *[a] Xin-Yu Wang,[a] Jin-Rong Li,[a] Jie Guo,[a] Gang Xiong,[a] Fu ding [a] and Ya-Guang Sun *[ab]

Received 20th June 2025,
Accepted 17th July 2025

DOI: 10.1039/d5ce00627a

rsc.li/crystengcomm

Transformation of carbon dioxide (CO_2) into high-value chemicals has attracted increasing attention because CO_2 is an abundant, inexpensive and non-toxic renewable carbon resource. Herein, a novel three-dimensional metal–organic framework, namely, $\{[Zn_4(\mu_4\text{-}O)(L)_4\cdot 4(H_2O)]\cdot 2(NO_3)\}_n$ (Zn-MOF), was synthesized under hydrothermal conditions using an azolium-based ligand, 1,3-bis(4-carboxybenzyl)-4-methyl-1*H* imidazolium chloride ($H_2L^+Cl^-$). Subsequently, Cu(I)-NHC@Zn-MOF was prepared by introducing N-heterocyclic carbine-Cu(I) active sites into the Zn-MOF using a post-synthesis modification (PSM) method, and it was characterized through powder X-ray diffraction (PXRD), X-ray photoelectron spectroscopy (XPS), transmission electron microscopy (TEM), thermogravimetric analysis (TGA) and inductively coupled plasma optical emission spectroscopy (ICP-OES). Cu(I)-NHC@Zn-MOF was successfully employed as a highly efficient catalyst for the C–H activated carboxylation of terminal alkynes with CO_2 (1 atm) under mild conditions, achieving an isolated yield of up to 98%. The catalyst exhibited excellent recyclability and maintained high activity over three consecutive cycles without losing its structural integrity. Additionally, the role of Cu(I)-NHC@Zn-MOF and the reaction mechanism were comprehensively discussed.

Introduction

Fixation and conversion of carbon dioxide (CO_2) into value-added chemicals are areas of intense research owing to their environmental and economic implications.[1,2] The direct carboxylation of CO_2 with terminal alkynes, which was initially reported by Inoue *et al.*[3] in 1994, has made remarkable progress in the straightforward synthesis of functionalized propiolic acids, which is a class of important compounds in the fields of medicinal chemistry and fine-chemicals. The carboxylation of terminal alkynes with CO_2 to yield the corresponding carboxylic acids proceeds using a base in the absence of a transition metal catalyst.[4,5] However, studies have shown that the presence of copper or silver salts can effectively promote the reactions even at low temperatures and ambient CO_2 pressures.[6–11] To overcome the drawbacks of homogeneous catalysts, heterogeneous catalysts have been developed for carboxylation reactions.[12–17] Heterogeneous catalysts are preferable alternatives owing to their recyclability, easy separation processes and reduced environmental impact due to minimized waste generation. However, either high catalyst loadings or synthetic complications limit the further application of these catalytic systems. Nevertheless, there is a necessity for further development of the design and synthesis of efficient, inexpensive, robust and reusable catalysts for such reactions.

N-Heterocyclic carbenes (NHCs) and their corresponding transition metal complexes, which arise from strong metal-NHC (NHC-M) bonding, are highly regarded in the field of catalysis.[18–20] Typically, the NHC-M moiety is synthesized from a metal ion and an NHC precursor, such as imidazolium, thiazolium, or triazolium salts, through deprotonation. Metal–organic frameworks (MOFs) exhibit exceptional potential as heterogeneous catalysts[21] owing to their unique organic–inorganic hybrid composition and polymeric architecture, which enable the incorporation of diverse active sites within their frameworks.[22,23] Furthermore, MOFs can be modified by incorporating specific ligands to further enhance their catalytic properties. This facilitates the fine-tuning of the chemical environment and introduction of novel catalytic functionalities.

[a] *Key Laboratory of Inorganic Molecule-Based Chemistry of Liaoning Province, Shenyang University of Chemical Technology, Shenyang 110142, China. E-mail: youlx@syuct.edu.cn*
[b] *Petrochemical Department, Liaoning Petrochemial College, Jinzhou 121000, China. E-mail: sunyaguang@syuct.edu.cn*

† Electronic supplementary information (ESI) available: CCDC 2465476. For ESI and crystallographic data in CIF or other electronic format see DOI: https://doi.org/10.1039/d5ce00627a

Recent studies have shown that NHC-M (Cu and Ag) can effectively catalyze the carboxylation of CO_2 with terminal alkynes. Thus far, transition metal NHC catalytic systems have been established for these reactions;[24–27] it is presumed that the free NHC site reacts with CO_2 to form NHC-carboxylate, and the alkynes are activated by NHC-M with the formation of metal acetylide as an intermediate. To the best of our knowledge, there are only a few reports on the carboxylation of terminal alkynes with CO_2 using MOF as the matrix and solid support for embedding the M-NHC moiety.[28]

In this study, a novel Zn-MOF, $\{[Zn_4(\mu_4\text{-}O)(L)_4{\cdot}4(H_2O)]{\cdot}2(NO_3)\}_n$, was synthesized using the NHC precursor 1,3-bis(4-carboxybenzyl)-4-methyl-1*H* imidazolium chloride ($H_2L^+Cl^-$) as the ligand. To decrease the cost of the catalyst, NHC sites were utilized to anchor Cu(I) ions, thereby yielding a copper-based MOF, Cu(I)-NHC@Zn-MOF, *via* a PSM method. The Cu(I)-embedded MOF served as a highly recyclable heterogeneous catalyst for the carboxylation of CO_2 with terminal alkynes under mild conditions.

Experimental

Materials and physico–chemical measurements

All the reagents were purchased from commercial suppliers and were used without further purification. FT-IR spectra were recorded using a Nicolet iS50 FTIR spectrometer using KBr particles. Powder X-ray diffraction (PXRD) of the samples was performed on a Smartlab9k polycrystalline X-ray diffractometer. Thermogravimetric analysis (TGA) was performed on a STA449C thermogravimetric analyzer. The temperature was increased from room temperature to 800 °C with a heating efficiency of 10 °C min^{-1} under a nitrogen atmosphere. X-ray photoelectron spectroscopy (XPS) was performed using a Model Axis Supra$^+$ X-ray photoelectron spectrometer. Inductively coupled plasma optical emission spectroscopy (ICP-OES) analysis was performed using an Agilent model 5110 inductively coupled plasma optical emission spectrometer. Transmission electron microscopy (TEM) images were obtained using a JEOL JEM-2800 scanning electron microscope. Energy chromatography dispersive X-ray spectroscopy (EDS) testing was performed using a SU8100 X-ray energy spectrometer. The obtained product was detected using ^{1}H NMR spectra recorded using an AVANCE III 500 MHz nuclear magnetic resonance spectrometer. Single crystal X-ray diffraction of the crystal was measured using an XtaLAB PROII diffractometer. The mass spectra were obtained using a Shimadzu GC-2030 AM.

Synthesis of Zn-MOF

1,3-Bis(4-carboxybenzyl)-4-methyl-1*H* imidazolium chloride ($H_2L^+Cl^-$) was obtained *via* the hydrolysis of 1,3-bis(methyl 4-formate)-4-methyl-1*H* imidazolium bromide ($(Me)_2L^+Br^-$) (details are provided in the ESI†). The mixture of $H_2L^+Cl^-$ (0.0105 g, 0.03 mmol) and $Zn(NO_3)_2{\cdot}6H_2O$ (0.0298 g, 0.1 mmol) in deionized water (7.0 mL) and *N*,*N*-dimethylacetamide (DMA) (2.0 mL) was sealed in a 20 mL glass sample bottle, ultrasonicated for 30 min, maintained under its own pressure at 100 °C for 72 h, and then allowed to cool naturally to room temperature. The product was then washed with the reaction solution and dried under vacuum to obtain colorless crystals (yield is 83% based on $Zn(NO_3)_2$). The IR data of $H_2L^+Cl^-$ and Zn-MOF are shown in Fig. S1 and S2.†

Synthesis of Cu-NHC-$(Me)_2$L and Cu(I)-NHC@Zn-MOF

Cu-NHC-$(Me)_2$L was prepared by reacting $(Me)_2L^+Br^-$ (0.3794 g, 1.0 mmol) with CuI (0.1905 g, 1.0 mmol) in acetonitrile (60 mL) for 48 h in the dark at room temperature under an argon atmosphere. After the completion of this reaction, the mixture was vacuum filtered, and the product was washed with ether and then vacuum dried to yield a dark brown solid.

Cu(I)-NHC@Zn-MOF was obtained by reacting Zn-MOF with CuI under similar reaction conditions (Scheme 1). The mixture of Zn-MOF (0.1870 g, 0.10 mmol), CuI (0.0190 g, 0.10 mmol) and acetonitrile (60 mL) was stirred at room temperature for 48 h. The solid obtained from the reaction mixture was subjected to vacuum filtration, followed by washing with acetonitrile, anhydrous methanol and diethyl ether. The solid was then vacuum dried to yield a white powder. The Cu content of Cu(I)-NHC@Zn-MOF was determined to be 0.29 wt% using ICP-OES.

Carboxylation reaction

A mixture of the terminal alkyne (1.0 mmol), base (3.0 mmol), solvent (10 mL) and catalyst (40, 50, 60 and 70 mg) was placed in a 25 mL reaction tube, and a standard atmospheric pressure of CO_2 was applied. The reaction tube was placed in an oil bath at 40, 50, 60, 70 and 80 °C and stirred for 12, 16, 19, 21 and 24 h. Subsequently, the mixture was transferred to a centrifuge tube, and 15 mL of deionized water was added for centrifugation. The centrifuged mixture was then transferred to a separation funnel and washed three times with 10 mL of dichloromethane. Then, 1 mol L^{-1} hydrochloric acid was added dropwise until the pH of the mixture was 1. The mixture was then extracted with ethyl acetate. The product was obtained by vacuum concentration and drying of the treated solution. By comparing the actual product weight with the theoretical weight for 1 mmol, the efficiency of the catalytic separation process can be assessed.

Crystal structure measurements

Crystallographic data were collected using an XtaLAB PROII diffractometer using an ω-2θ scanning technique by applying a graphite-monochromatized Mo Kα radiation (λ = 0.71073 Å). The data were corrected for empirical absorption using the SADABS program.[29] All structures were determined *via* the direct method and optimized using full matrix least squares on F^2 using the SHELXTL crystallography software package.[30] All non-hydrogen atoms were anisotropically refined. Hydrogen atoms were placed at the calculated positions and refined using horseback riding mode. The

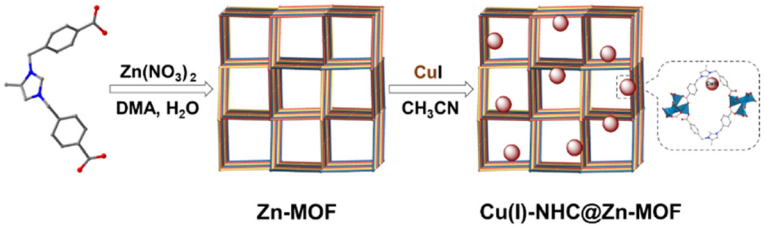

Scheme 1 Synthesis route of Cu(I)-NHC@Zn-MOF.

crystal and structure refinement data of Zn-MOF (CCDC: 2465476) are provided in Table S1.†

Results and discussion

Crystal structure

Single crystal X-ray diffraction analysis demonstrated that Zn-MOF belonged to the tetragonal system, *I*41/*a* space group. As illustrated in Fig. S3,† Zn(II) was coordinated with four oxygen atoms from a central μ_4-O atom (O1) and three L^- ligands. The L^- ligand exhibited the same coordination pattern as that of the Zn-MOF: (κ_1-κ_1-μ_2)-(κ_1-μ_1)-μ_3 (Fig. 1a). The μ_4-O linked four Zn(II) ions, which were bridged *via* the carboxyl groups of the ligands to build the [Zn_4(μ_4-O)$(COO)_4$] secondary building unit (SUB), to form a tetrapyramidal structure (Fig. 1b). Two adjacent SUBs were alternately connected by two L^- ligands to expand the three-dimensional framework (Fig. 1c). Furthermore, a triple interpenetrating framework was formed owing to the low connection topology and long organic ligand of the Zn-MOF (Fig. 1d and e).

Powder X-ray diffraction (PXRD) and thermogravimetric analysis (TGA)

Powder X-ray diffraction (PXRD) was conducted to confirm the phase purity of Zn-MOF (Fig. S4†). All main peaks of the single crystal structure corresponded well with those of the as-synthesized Zn-MOF. The crystal maintained its complete structure during the preparation of the Cu(I)-NHC@Zn-MOF, thereby confirming that the framework exhibited excellent phase purity and homogeneity. Thermogravimetric analysis (TGA) of Zn-MOF and Cu(I)-NHC@Zn-MOF was conducted. The initial weight loss of Zn-MOF that occurred between 40 °C and 130 °C, was approximately 4.86%, which corresponded to the loss of free water molecules (calculated: 3.85%). Zn-MOF remained thermally stable up to 300 °C and decomposed at higher temperatures. The TGA curve of Cu(I)-NHC@Zn-MOF was similar to that of Zn-MOF, indicating its excellent thermal stability (Fig. S5†).

^{1}H nuclear magnetic resonance (^{1}H NMR) spectroscopy

To evaluate the feasibility of incorporating Cu(I) into Zn-MOF, Cu-NHC-$(Me)_2$L was prepared by reacting $(Me)_2L^+Br^-$ with CuI. Fig. 2 shows the ^{1}H NMR spectra of $(Me)_2L^+Br^-$ and Cu(I)-NHC-$(Me)_2$L. The disappearance of the peak at 9.4 ppm, which corresponded to the *C*2 proton on the imidazolium ring of $(Me)_2L^+Br^-$, confirmed the successful formation of NHC-Cu(I) structure.[31]

X-ray photoelectron spectroscopy (XPS)

X-ray photoelectron spectroscopy (XPS) studies provided further insights into the chemical structures before and after Cu(I) loading. The presence of the expected elements (Br, C, N and O for $(Me)_2L^+Br^-$; C, N, O, I and Cu for Cu-

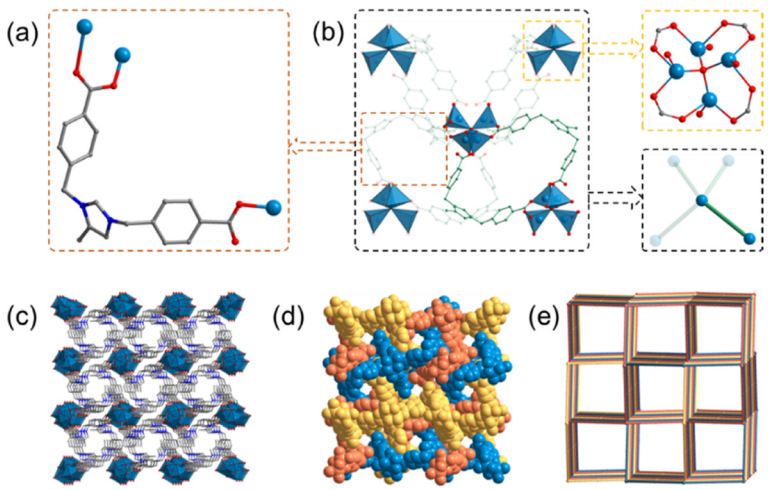

Fig. 1 (a) Coordination mode of the L^- ligand; (b) [Zn_4(μ_4-O)$(COO)_4$] secondary building units connected by L^- ligands; (c) single 3D framework; (d) 3-fold interpenetrated network; and (e) illustration of the 3D topology of the Zn-MOF.

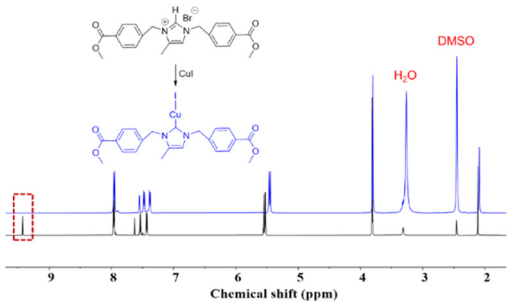

Fig. 2 ^{1}H NMR spectra of $(Me)_2L^+Br^-$ (black) and Cu(I)-NHC-$(Me)_2L$ (blue).

NHC-$(Me)_2$L, C, N, O and Zn for Zn-MOF; and C, N, O, I, Zn and Cu for Cu(I)-NHC@Zn-MOF) was confirmed by the survey spectra (Fig. S6 and S7†). As shown in Fig. 3a and b, the binding energies of N 1s at 401.1 eV were assigned to the C=N bond within the imidazolium ring. After the formation of the C–Cu bond, the N 1s peak of Cu-NHC-$(Me)_2$L decreased to 400.3 eV, and a new peak was formed at 398.8 eV for Cu(I)-NHC@Zn-MOF. The significant reduction was due to the transformation of the imine C=N bond to the enamine C–N bond through Cu(I) coordination at the *C*2 site.[32] Fig. 3c shows the binding energies of Cu 2p for the prepared Cu(I)-NHC@Zn-MOF and Cu(I)-NHC-$(Me)_2$L. For the Cu(I)-NHC@Zn-MOF, the distinct peaks at 932.8 and 952.5 eV are assigned to Cu $2p_{3/2}$ and Cu $2p_{1/2}$, respectively. These two peaks also maintained similar positions in Cu-NHC-$(Me)_2$L. Although the observed binding energy varied slightly for each sample, the difference between the two peaks was constantly maintained at 19.9 eV. This indicated the presence of Cu(I), which was in accordance with the results from Fig. S6 and S7.† In addition, the XPS spectrum of Cu 2p for the recycled catalyst is shown in Fig. 3d; notably, the two distinct peaks at 932.0 and 952.5 eV were assigned to Cu $2p_{3/2}$ and Cu $2p_{1/2}$, respectively.[33]

Transmission electron microscopy (TEM)

The morphology of Cu(I)-NHC@Zn-MOF was examined using the transmission electron microscopy (TEM), as shown in Fig. 4a. The TEM image was composed of irregular blocks of massive particles, and the energy-dispersive X-ray spectroscopy (EDS) results confirmed the presence of Cu, Zn, C, N and O elements in Cu(I)-NHC@Zn-MOF (Fig. S8†). Furthermore, the elemental mapping images indicated a homogeneous dispersion of Cu, Zn, C, N and O elements, which illustrated the successful synthesis of Cu(I)-NHC@Zn-MOF (Fig. 4b–f).

Catalytic activity

Following the determination of the structure, the role of Cu(I)-NHC@Zn-MOF in the carboxylation reaction of CO_2 with terminal alkynes was explored by introducing 1 atm CO_2 and varying the solvents, bases, reaction times and catalyst amounts at different temperatures (Table S2†). The optimum reaction conditions were as follows: Cs_2CO_3 as the base, dimethyl sulfoxide (DMSO) as the solvent, and a reaction time of 24 h at 60 °C with Cu(I)-NHC@Zn-MOF (60 mg); these conditions offered an optimal yield of 95% (Entry 1). However, when alternative solvents, namely, MeOH, CH_3CN, tetrahydrofuran (THF) and toluene, were employed, the yield was found to be considerably lower than that achieved using DMSO (Entries 1, 14–17). Furthermore, when reacted with different bases, including K_2CO_3, KOH, Na_2CO_3 and NaOH, only minimal yields were

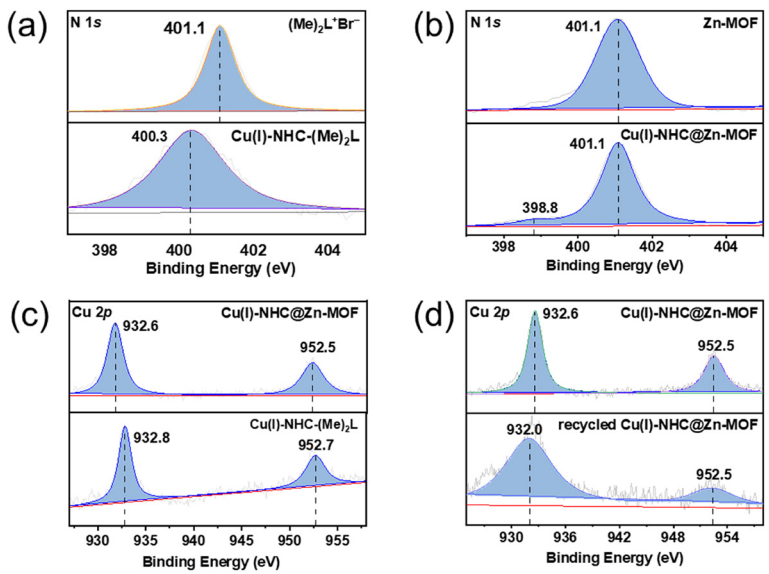

Fig. 3 (a) XPS spectra of N 1s in Cu(I)-NHC-$(Me)_2$L and $(Me)_2L^+Br^-$; (b) N 1s in Zn-MOF and Cu(I)-NHC@Zn-MOF; (c) Cu 2p in Cu(I)-NHC@Zn-MOF and Cu(I)-NHC-$(Me)_2$L; (d) Cu 2p in Cu(I)-NHC@Zn-MOF and recycled Cu(I)-NHC@Zn-MOF.

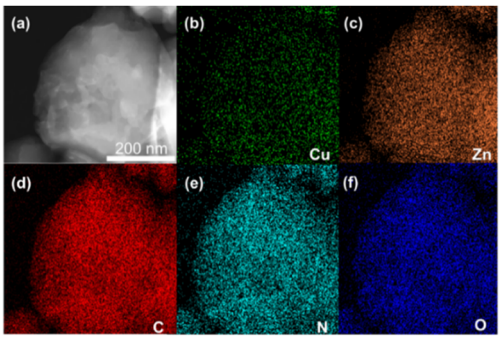

Fig. 4 (a) TEM image of Cu(I)-NHC@Zn-MOF and (b–f) elemental mappings of Cu, Zn, C, N and O atoms.

obtained (Entries 1, 18–21). It was observed that an increase in the reaction temperature resulted in a gradual enhancement in the yield up to 60 °C, after which a decline was found to occur (Entries 1–5). This phenomenon can be attributed to the instability of the cuprous alkynide intermediate formed during the reaction, which causes decarboxylation at high temperature.[34] The absence of Cu(I)-NHC@Zn-MOF or Zn-MOF as a catalyst resulted in no observable product (Entries 6, 22). The highest product yield was observed when 60 mg of catalyst was used, and increasing or decreasing the amount of catalyst led to a decrease in the product yield (Entries 1, 7–9). When the reaction time was shortened, the yield of the reaction was gradually reduced (Entries 1, 10–13). Notably, Cu(I)-NHC@Zn-MOF displayed superior catalytic activity in comparison to previously reported catalysts, which are known for their use in the carboxylation of terminal alkynes with CO_2.[25,35–38]

To gain deeper insights into the catalytic mechanism, a series of control experiments were carried out (Table 1). As shown in Entry 1, DMSO absorbed CO_2, thereby promoting the reaction.[39] When Zn-MOF was added, the observed product yield increased from 7% to 33% (Entry 2). This enhancement in the yield could be ascribed to the NHC structure formed by the imidazolium in Zn-MOF in the presence of Cs_2CO_3. NHC combined with CO_2 to form NHC carboxylate (NHC-CO_2), which in turn promoted the carboxylation of terminal alkynes with CO_2.[24] The use of CuI as a catalyst resulted in a 67% product yield (Entry 3), indicating the efficacy of Cu(I) in this reaction.[40] In contrast to Entry 3, the addition of Zn-MOF (60 mg) resulted in the a product yield of 74%. Here, it could be hypothesized that the generation of some Cu(I)-NHC@Zn-MOF during the stirring process further enhanced the catalytic performance (Entry 4). Subsequently, when Cu(I)-NHC-$(Me)_2$L was chosen

Table 1 Carboxylation of CO_2 with phenylacetylene under different reaction conditions

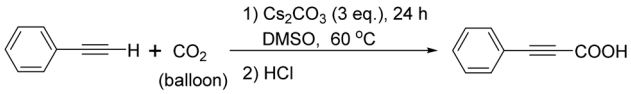

Entry	Catalyst (0.27 mol% Cu)	Yield[a] (%)
1[b]	Cu(I)-NHC@Zn-MOF	7
2[c]	Cu(I)-NHC@Zn-MOF	33
3	CuI	67
4	CuI/Zn-MOF (60 mg)	74
5	Cu(I)-NHC-$(Me)_2$L	80

[a] Isolated yield. [b] CO_2 (balloon) was introduced for 2 h, then the balloon was removed, and Cu(I)-NHC@Zn-MOF was added and reacted for 24 h. [c] Zn-MOF (200 mg) was added in contrast to Entry 1.

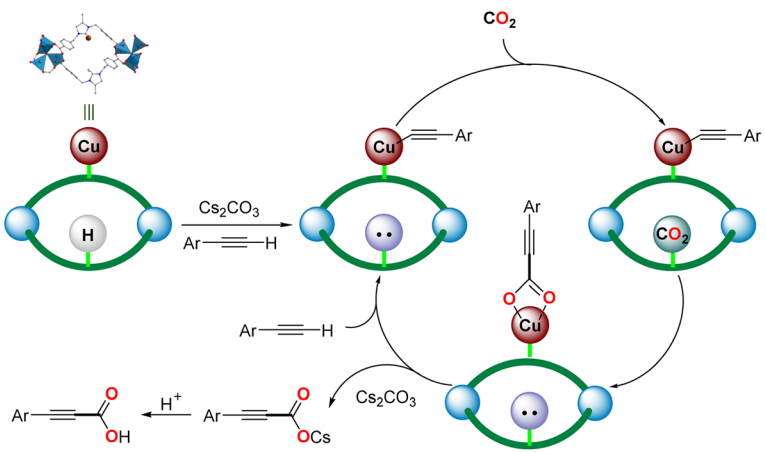

Scheme 2 Possible mechanism of the carboxylation of terminal alkynes with CO_2.

for the reaction, a product yield of 80% (Entry 5) was observed, indicating that Cu(I)-NHC active site exhibited enhanced catalytic activity when combined with Cu(I). However, it should be noted that Cu-NHC-$(Me)_2$L is a homogeneous catalyst and cannot be recycled. Heterogeneous Cu(I)-NHC@Zn-MOF was then prepared by the PSM method, which offered a product yield of 95% (Table S2,† Entry 1).

Based on the aforementioned results and previous reports,[3,4,12,26,41] a possible mechanism for the catalytic carboxylation of terminal alkynes with CO_2 was proposed (Scheme 2). Initially, the proton at the *C*2 position of the imidazolium structure was removed, resulting in the formation of an NHC structure. Concurrently, Cu(I)-NHC in the Zn-MOF underwent a reaction with terminal alkyne and Cs_2CO_3, yielding alkyne-copper intermediates.[3,4] Subsequently, NHC attacked the carbon atom of the CO_2 to form the NHC carboxylate (NHC-CO_2);[12,26,41] this was consistent with the capture ability of carbon dioxide by the MOF (Table 1, Entry 2). NHC-CO_2 then coordinated with a nearby copper center, inducing the nucleophilic carbanion of the alkyne to attack the carboxylic carbon. The formation of a new C–C bond then occurred, and the CO_2 unit was transferred from NHC to the copper center to form a copper arylpropionate intermediate, which then reacted with another terminal alkyne and Cs_2CO_3 to release cesium propionate while regenerating NHC and the copper acetylene intermediate. After the reaction, cesium arylpropionate was acidified using hydrochloric acid to obtain an arylpropiolic acid product.

The effects of different substituents on the yield were examined under the optimum conditions (Table 2). Results showed that Cu(I)-NHC@Zn-MOF exhibited excellent catalytic efficiency for substrates with both electron donor groups (H_3CO– and CH_3–) and electron withdrawing groups (F–, Cl–, and CN–), and the yield of the products reached more than 90%. Additionally, Cu(I)-NHC@Zn-MOF was applicable to a wide range of functional groups.

Table 2 Cu(I)-NHC@Zn-MOF-catalyzed carboxylation of CO_2 with different terminal alkynes[a]

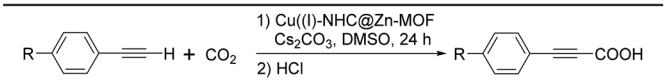

Entry	R	Product	Yield[b] (%)
1	F	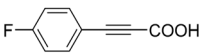	98
2	Cl	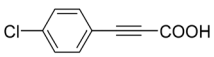	98
3	H	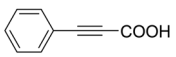	95
4	CH_3	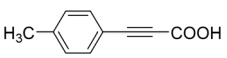	95
5	CN	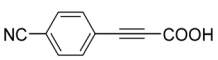	94
6	OCH_3	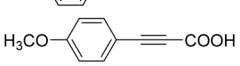	90

[a] Reaction conditions: alkyne (1.0 mmol), Cs_2CO_3 (3.0 mmol), CO_2 (balloon pressure), Cu(I)-NHC@Zn-MOF (60.0 mg, 0.27 mol%), DMSO (10.0 mL), 60 °C. [b] Isolated yield.

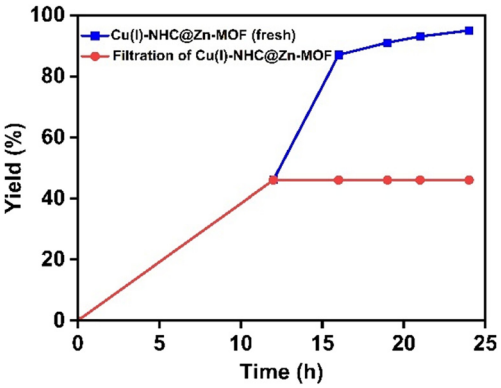

Fig. 5 Plots of the yield *versus* time for the carboxylation reaction of phenylacetylene with CO_2 in the presence (blue) and removal (red) of the Cu(I)-NHC@Zn-MOF *via* filtration after a reaction time of 12 h.

To determine the heterogeneous catalytic performance of Cu(I)-NHC@Zn-MOF, a hot filtration experiment was conducted in accordance with the standard procedure. The yield was 46% after 12 h of reaction, and there was no increase in yield after the removal of the catalyst (Fig. 5), demonstrating that no Cu(I) was leached from the catalyst to the filtrate after the catalyst was filtered.

As shown in Fig. 6, the product yield could still reach 89% after 3 cycles under the optimum reaction conditions. This indicates that Cu(I)-NHC@Zn-MOF was efficiently recovered with almost no loss of activity after four consecutive runs. The PXRD pattern (Fig. S4†) revealed that the uniform crystalline state of the Zn-MOF backbones was maintained during the catalytic cycle run with Cu(I)-NHC@Zn-MOF. In addition, the XPS spectrum of Cu 2p for the recycled catalyst is shown in Fig. 3d, and the two distinct peaks at 932.0 and 952.5 eV are assigned to Cu $2p_{3/2}$ and Cu $2p_{1/2}$, respectively. However, with the increase in the catalytic frequency, the yield of the catalytic products decreased gradually.

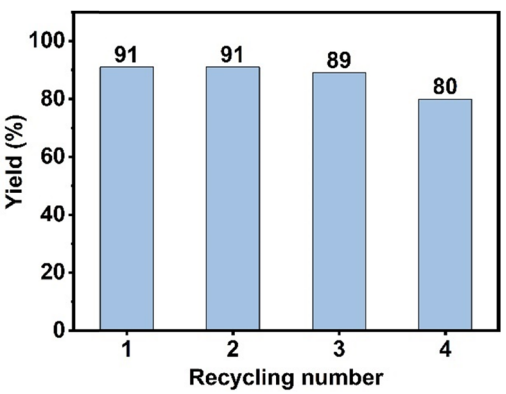

Fig. 6 Recycling of Cu(I)-NHC@Zn-MOF used in the carboxylation reaction of phenylacetylene and CO_2.

Conclusions

In summary, a non-noble metal, bifunctional heterogeneous catalyst (Cu(I)-NHC@Zn-MOF) was synthesized *via* a post-modification synthesis method by introducing a Cu(I)-NHC moiety into a Zn-MOF. The stable and efficient catalyst exhibited highly selectivity and recyclability in the carboxylation of terminal alkynes with carbon dioxide, and the high catalytic activity was maintained after three cycles of regeneration without any loss in structural integrity. The synergistic cooperation between the Cu(I)-NHC active site and the NHC-CO_2 motif was clearly confirmed in the reaction of CO_2 and terminal alkynes catalyzed by Cu(I)-NHC@Zn-MOF. This work, therefore, provides a promising strategy for the design of noble metal-free N-heterocyclic carbene-metal modified metal–organic frameworks for highly efficient conversion of CO_2 into high-value chemicals.

Data availability

The authors confirm that the data supporting the findings of this study are available within the article and its ESI.†

Conflicts of interest

There are no conflicts of interest to declare.

Acknowledgements

This work was supported by the Qualified Approval Project of Shenyang University of Chemical Technology (LDB2022002) and the Science and Technology Program Project of Liaoning Province (2023JH1/10400039).

Notes and references

1 Y. Wang, J. X. Wei, H. L. Tang, L. H. Shao, L. Z. Dong, X. Y. Chu, Y. X. Jiang, G. L. Zhang, F. M. Zhang and Y. Q. Lan, *Nat. Commun.*, 2024, **15**, 8818.
2 J. Liang, Y. B. Huang and R. Cao, *Coord. Chem. Rev.*, 2019, **378**, 32–65.
3 Y. Fukue, S. Oi and Y. Inoue, *J. Chem. Soc., Chem. Commun.*, 1994, 2091.
4 D. Y. Yu and Y. G. Zhang, *Green Chem.*, 2011, **13**, 1275–1279.
5 W. H. Wang, X. J. Feng, K. Sui, D. Q. Fang and M. Bao, *J. CO2 Util.*, 2019, **32**, 140–145.
6 T. Wendling, E. Risto, T. Krause and L. J. Gooßen, *Chem. - Eur. J.*, 2018, **24**, 6019–6024.
7 D. Yu and Y. Zhang, *Proc. Natl. Acad. Sci. U. S. A.*, 2010, **107**, 20184–20189.
8 W. Z. Zhang, W. J. Li, X. Zhang, H. Zhou and X. B. Lu, *Org. Lett.*, 2010, **12**, 4748–4751.
9 L. J. Gooßen, N. Rodríguez, F. Manjolinho and P. P. Lange, *Adv. Synth. Catal.*, 2010, **352**, 2913–2917.
10 X. Zhang, W. Z. Zhang, X. Ren, L. L. Zhang and X. B. Lu, *Org. Lett.*, 2011, **13**, 2402–2405.
11 M. Arndt, E. Risto, T. Krause and L. J. Gooßen, *ChemCatChem*, 2012, **4**, 484–487.
12 D. Yu, M. X. Tan and Y. Zhang, *Adv. Synth. Catal.*, 2012, **354**, 969–974.
13 X. H. Liu, J. G. Ma, Z. Niu, G. M. Yang and P. Cheng, *Angew. Chem., Int. Ed.*, 2015, **54**, 988–991.
14 R. A. Molla, K. Ghosh, B. Banerjee, M. A. Iqubal, S. K. Kundu, S. M. Islam and A. Bhaumik, *J. Colloid Interface Sci.*, 2016, **477**, 220–229.
15 M. Trivedi, B. Bhaskaran, A. Kumar, G. Singh, A. Kumar and N. P. Rath, *New J. Chem.*, 2016, **40**, 3109–3118.
16 G. Xiong, B. Yu, J. Dong, Y. Shi, B. Zhao and L. N. He, *Chem. Commun.*, 2017, **53**, 6013–6016.
17 Z. Wu, Q. Liu, X. Yang, X. Ye, H. Duan, J. Zhang, B. Zhao and Y. Huang, *ACS Sustainable Chem. Eng.*, 2017, **5**, 9634–9639.
18 M. N. Hopkinson, C. Richter, M. Schedler and F. Glorius, *Nature*, 2014, **510**, 485–496.
19 S. P. Nolan and C. S. J. Cazin, *Thieme*, 2017, **1**, 1072.
20 E. Peris, *Chem. Rev.*, 2017, **118**, 9988–10031.
21 L. X. You, B. Y. Ren, Y. K. He, S. J. Wang, Y. G. Sun, V. Dragutan, G. Xiong and F. Ding, *J. Mol. Struct.*, 2024, **1304**, 137687.
22 A. Corma, H. García and F. X. L. i. Xamena, *Chem. Rev.*, 2010, **110**, 4606–4655.
23 M. Yoon, R. Srirambalaji and K. Kim, *Chem. Rev.*, 2012, **112**, 1196–1231.
24 J. B. Shi, Q. Bu, B. Y. Liu, B. Dai and N. Liu, *J. Org. Chem.*, 2020, **86**, 1850–1860.
25 Y. Li, Y. Dong, J. L. Kan, X. Wu and Y. B. Dong, *Org. Lett.*, 2020, **22**, 7363–7368.
26 S. Li, J. Sun, Z. Zhang, R. Xie, X. Fang and M. Zhou, *Dalton Trans.*, 2016, **45**, 10577–10584.
27 F. Manjolinho, M. Arndt, K. Gooßen and L. J. Gooßen, *ACS Catal.*, 2012, **2**, 2014–2021.
28 L. X. You, T. C. Han, J. R. Li, J. Guo, G. Xiong, F. ding and Y. G. Sun, *J. Environ. Chem. Eng.*, 2025, **13**, 11678.
29 C. B. Hübschle, G. M. Sheldrick and B. Dittrich, *J. Appl. Crystallogr.*, 2011, **44**, 1281–1284.
30 G. M. Sheldrick, *Acta Crystallogr., Sect. A: Found. Crystallogr.*, 2008, **64**, 112–122.
31 Q. Teng, W. Liu, Y. Zhao, L. Zhang, H. Jin, Q. Meng and G. Frison, *Inorg. Chem.*, 2024, **63**, 21806–21809.
32 A. M. Ferraria, A. P. Carapeto and A. M. B. do Rego, *Vacuum*, 2012, **86**, 1988–1991.
33 Z. Zhang, H. Gao, H. Wu, Y. Qian, L. Chen and J. Chen, *ACS Appl. Nano Mater.*, 2018, **11**, 6463–6476.
34 R. Bu, L. Zhang, L. L. Gao, W. J. Sun, S. L. Yang and E. Q. Gao, *Mol. Catal.*, 2021, **499**, 111319.
35 G. Shi, W. Xu, J. Wang, Y. Yuan, S. Chaemchuen and F. Verpoort, *J. CO2 Util.*, 2020, **39**, 101177.
36 R. J. Wei, M. Xie, R. Q. Xia, J. Chen, H. J. Hu, G. H. Ning and D. Li, *J. Am. Chem. Soc.*, 2023, **145**, 22720–22727.
37 L. Zhang, R. Bu, X. Y. Liu, P. F. Mu and E. Q. Gao, *Green Chem.*, 2021, **23**, 7620–7629.

38 J. Shi, L. Zhang, N. Sun, D. Hu, Q. Shen, F. Mao, Q. Gao and W. Wei, *ACS Appl. Mater. Interfaces*, 2019, **11**, 28858–28867.
39 H. A. Shirazizadeh and A. Haghtalab, *Fluid Phase Equilib.*, 2021, **528**, 112845.
40 W. J. Wang, Z. H. Sun, S. C. Chen, J. F. Qian, M. Y. He and Q. Chen, *Appl. Organomet. Chem.*, 2021, **35**, e6288.
41 H. Díaz Velázquez, Z. X. Wu, M. Vandichel and F. Verpoort, *Catal. Lett.*, 2017, **147**, 463–471.